



저작자표시-비영리-변경금지 2.0 대한민국

이용자는 아래의 조건을 따르는 경우에 한하여 자유롭게

- 이 저작물을 복제, 배포, 전송, 전시, 공연 및 방송할 수 있습니다.

다음과 같은 조건을 따라야 합니다:



저작자표시. 귀하는 원저작자를 표시하여야 합니다.



비영리. 귀하는 이 저작물을 영리 목적으로 이용할 수 없습니다.



변경금지. 귀하는 이 저작물을 개작, 변형 또는 가공할 수 없습니다.

- 귀하는, 이 저작물의 재이용이나 배포의 경우, 이 저작물에 적용된 이용허락조건을 명확하게 나타내어야 합니다.
- 저작권자로부터 별도의 허가를 받으면 이러한 조건들은 적용되지 않습니다.

저작권법에 따른 이용자의 권리는 위의 내용에 의하여 영향을 받지 않습니다.

이것은 [이용허락규약\(Legal Code\)](#)을 이해하기 쉽게 요약한 것입니다.

[Disclaimer](#)

**Novel derivatives of
neohesperidin dihydrochalcone inhibit
adipogenic differentiation of
human adipose-derived stem cells
through the Nrf2 pathway**

Hee-Taik Kang

Department of Medicine

The Graduate School, Yonsei University

**Novel derivatives of
neohesperidin dihydrochalcone inhibit
adipogenic differentiation of
human adipose-derived stem cells
through the Nrf2 pathway**

Hee-Taik Kang

Department of Medicine

The Graduate School, Yonsei University

**Novel derivatives of
neohesperidin dihydrochalcone inhibit
adipogenic differentiation of
human adipose-derived stem cells
through the Nrf2 pathway**

Directed by Professor John A. Linton

Doctoral Dissertation
submitted to the Department of Medicine
the Graduate School of Yonsei University
in partial fulfillment of the requirements for the degree
of Doctor of Philosophy

Hee-Taik Kang

June 2018

This certifies that the Doctoral
Dissertation of Hee-Taik Kang
is approved.

Thesis Supervisor: John A. Linton

Thesis Committee Member#1: Duk-Chul Lee

Thesis Committee Member#2: Jong Hun Lee

Thesis Committee Member#3: Byung-Wan Lee

Thesis Committee Member#4: Je-Wook Yu

The Graduate School
Yonsei University

June 2018

ACKNOWLEDGEMENTS

I would like to express profound gratitude to my supervisor, Professor John A. Linton, for his unlimited support and supervision and valuable suggestions throughout this research work. This research can be successfully made by Professor Linton's sincere advice and moral supervision. I also deeply appreciate the encouragement of Professor Duk-Chul Lee who always makes me awake and do my best. In addition, I am really grateful to Professor Jong Hun Lee, Byung-Wan Lee, and Je-Wook Yu for their insightful and scientific suggestions throughout this work. Valuable discussion and advices of all thesis committee members including Professor John A. Linton allowed my research to take one step further.

I would like to express appreciation to Professor Jae-Yong Shim, Yong-Jae Lee, and Hye-Ree Lee. They always help me to grow into a useful family physician, listen to difficult situation and try to solve it. Their advice and guidance led me to grow up as a researcher, a doctor, and a professor. They are my true senior physicians, teachers, and companions.

I owe my parents and sisters for their love and support throughout my life. They have given up what they had and could have for me. I will live with my gratitude in my heart for the rest of my life. A special word of thanks is certainly in order for my beloved wife, Eun-Young Jang. She always supported me with her understanding from the heart and encouraged for me not to abandon my dream. Most especially, I thanks to my beloved and cute daughters, Ga-Byul, Ga-On, and Ga-Eul. My dear children, you are my hope and my life, itself. You always grow me up and encourage me to do my best without giving up even in any difficult situations. This thesis is dedicated to my children, Ga-Byul, Ga-On, and Ga-Eul, my lovely wife, Eun-Young Jang, my parents and sisters. They have been my inspiration and motivation throughout this work and my life.

Hee-Taik Kang

<TABLE OF CONTENTS>

ABSTRACT	1
I. INTRODUCTION	4
II. MATERIALS AND METHODS	9
1. Chemicals and reagents	9
2. Cell culture	9
3. Synthesis of neohesperidin dihydrochalcone (NHDC) derivatives	10
4. Cell viability of human adipose-derived stem cells (hASCs) with NHDC derivatives	11
5. <i>In vitro</i> adipogenic differentiation of hASCs and NHDC derivatives treatment	11
6. Measurement of lipid accumulation during adipogenic differentiation of hASCs with/without NHDC and its derivatives	12
7. Reactive oxygen species (ROS) measurement	13
8. Quantitative reverse transcriptase-polymerase chain reaction (qRT-PCR) analysis	14
9. Western blot analysis	15
10. Statistical analysis	16
III. RESULTS	16
1. Chemistry	16
2. Cell viability of hASCs by NHDC and derivatives treatment	23
3. Inhibition effects of NHDC derivatives on the adipogenic differentiation of hASCs	25
4. Anti-lipogenesis effect of NHDC derivatives during adipogenic differentiation of hASCs	27
5. Effect of NHDC and derivatives on ROS generation during adipogenic differentiation of hASCs	31
6. Induction of Nrf2 and its downstream antioxidant enzymes by NHDC and derivatives in adipogenic differentiation of hASCs	33

IV. DISCUSSION	35
V. CONCLUSION	39
REFERENCES	40
ABSTRACT(IN KOREAN)	46

LIST OF FIGURES

Figure 1. Preventive effects of NHDC derivatives on adipogenic differentiation of hASCs	8
Figure 2. Synthetic scheme of NHDC derivatives	10
Figure 3. Structures of synthesized NHDC and its derivatives	18
Figure 4. Viability of hASCs in the presence of NHDC and its derivatives	24
Figure 5. Effect of NHDC and its derivatives on adipogenic differentiation	26
Figure 6. Changes in expression of adipogenic and lipogenic markers over time	28
Figure 7. Effects of NHDC derivatives on lipogenesis during the adipogenic differentiation	30
Figure 8. ROS-mediated adipogenic differentiation in hASCs	32
Figure 9. Activation of Nrf2 pathway by NHDC and its derivatives in hASCs	34

ABSTRACT

**Novel derivatives of neohesperidin dihydrochalcone
inhibit adipogenic differentiation of human adipose-derived stem cells
through the Nrf2 pathway**

Hee-Taik Kang

*Department of Medicine
The Graduate School, Yonsei University*

(Directed by Professor John A. Linton)

Background: Obesity is a global epidemic. The pathogenesis of obesity is complicated and interacted with multiple factors including distorted adipogenesis through oxidative stress and inflammation as well as excessive calorie intake and physical inactivity. Reactive oxygen species (ROS) are involved to adipogenic differentiation. Neohesperidin as one of strong antioxidants has a significant free radical scavenging activity and anti-inflammatory activity. There is lack of studies to elucidate that neohesperidin dihydrochalcone (NHDC) and its derivatives can suppress adipogenic differentiation and obesity development.

Purpose: The main objective of this study is to determine the inhibitory effects of NHDC and its derivatives on *in vitro* adipogenic differentiation of human adipose-derived stem cells (hASCs).

Materials and Methods: hASCs were cultured with supplementation of growth factor and L-glutamine. The culture medium was changed every 3 days and the cells were used in early passages (fourth to seventh). The cytotoxicity of NHDC and its derivatives on hASCs was estimated. hASCs were cultured in proliferation and differentiation medium in the presence or absence of NHDC or derivatives, and experimental groups are as follows: Control group, no NHDC and derivatives + proliferative media only; Differentiation group, no NHDC and derivatives + proliferation and differentiation media; Sample group, NHDC or derivatives + proliferation and differentiation media. The accumulation of intracellular lipid droplets was evaluated using Oil Red O staining. The expression of adipogenic marker at RNA level and protein level were assessed by RT-PCR and Western blotting, respectively.

Results: The inhibition of adipogenic differentiation of hASC was tested against NHDC and its derivatives (compounds 9 and 12). In the NHDC treated group, slightly reduced Oil Red O staining was observed compared with the differentiated group. The amount of lipid accumulation decreased in the order of compounds 12 and 9. The expression of peroxisome proliferator-activated receptor- γ (PPAR- γ) in compound 9 and 12 treated groups was decreased by 46.7% and 70% respectively, compared to adipogenic differentiation group. Expression of fatty acid synthase (FAS) was decreased by 51.6% and 38.7% by compounds 9 and 12, respectively. Additionally, compounds 9 and 12 reduced the expression of sterol regulatory element-binding protein-1 (SREBP-1) by 65.7% and 60%, respectively. Although the fluorescent

intensity of ROS in experimental groups including NHDC and compound 12 were not dramatically weaker than differentiation group, compound 9 showed strong reduction of ROS. Expression of nuclear factor-erythroid-2-related factor 2 (Nrf2) protein did not show any statistically significant difference in the group treated with NHDC and compound 9, but significant increased expression was observed in the group treated with compound 12 compared to the differentiation group. Relatively, the expression of heme oxygenase 1 (HO-1) and NAD(P)H:quinine oxidoreductase-1 (NQO-1) was significantly increased in the NHDC-treated experimental group.

Conclusions: NHDC derivatives inhibited adipogenic differentiation in hASC by regulation of ROS through the activation of Nrf2 pathway. NHDC derivatives, having strong effects of Nrf2 activation and ROS reduction in hASC could be a potential therapeutic tool to overcome obesity. Especially, compound 9 having stronger Nrf2 activation activity showed higher reduction of ROS production.

Key words : neohesperidin; adipogenesis; stem cell; reactive oxygen species; Nrf2

**Novel derivatives of neohesperidin dihydrochalcone
inhibit adipogenic differentiation of human adipose-derived stem cells
through the Nrf2 pathway**

Hee-Taik Kang

*Department of Medicine
The Graduate School, Yonsei University*

(Directed by Professor John A. Linton)

I. INTRODUCTION

Obesity is a global epidemic. It is associated with numerous disorders, such as diabetes, metabolic syndrome, renal impairments, cancers, and other cardiovascular diseases, resulting in inflation of medical expenditures and significant public health burdens.^{1,2,3} Several studies have predicted that future obesity prevalence would gradually increase, even though its prevalence has levelled off or been stabilized in several developed countries.^{4,5} The pathogenesis of obesity is complicated and interacted with multiple factors including distorted adipogenesis through oxidative stress and inflammation as well as excessive calorie intake and physical inactivity.⁶

Human bone marrow-derived mesenchymal stem cells (hMSCs), multipotent adult stem cells, have the ability to differentiate into three typical lineages such as

adipocytes, osteoblasts and chondrocytes.⁷ Adipose-derived stem cells (ASCs) are mesenchymal stem cells (MSCs) that are obtained from abundant adipose tissue.^{8,9} Increased fat mass is caused by an increase in size (hypertrophy) and number (hyperplasia) of adipocytes. Excessive calorie intake over expenditure results in energy accumulation and hypertrophy of adipocytes through increased volume of cytoplasm and cell membrane area. In addition, the recruitment and proliferation of preadipocytes that have been derived from MSC, especially adipose-derived stem cells could lead to chronic inflammation, which results in various pathogenic burdens.^{10,11}

Reactive oxygen species (ROS) are involved to the modulation of cell functions, such as proliferation, differentiation, and survival.¹² ROS derived from nicotinamide adenine dinucleotide phosphate (NADPH) oxidase in mitochondria appear to have a role in adipogenic differentiation.^{13,14} It was demonstrated that the increased ROS induced adipogenesis in adipocyte was eliminated by an NADPH oxidase inhibitor.¹⁴ On the other hand, it was reported that ROS might up-regulate the CCAAT-enhancer binding protein- α (C/EBP- α) and peroxisome proliferator-activated receptor- γ (PPAR- γ), which resulted in adipogenesis in hMSC.¹⁵ Sterol regulatory element-binding proteins (SREBPs), the common lipogenic transcription factors, regulated the expression of lipogenic enzymes including fatty acid synthase (FAS).¹⁶ The activation of SREBP was used as a marker of the lipogenesis status of the cell and had synergistic effect with PPAR- γ on lipogenesis.^{17,18} Oxidative stress leads to adipogenesis through up-regulation of C/EBP- α , PPAR- γ , SREBP and FAS. If it is

possible to effectively regulate the ROS that induces adipogenic differentiation and lipogenesis, it is deduced that obesity can be prevented.

Nuclear factor-erythroid-2-related factor 2 (Nrf2) is an important cytoprotective transcription factor that induces the expression of phase II enzymes and phase II detoxifying enzymes, resulting in protective action on oxidative stress and reactive carcinogens.¹⁹ Once cells are exposed to oxidative stress, an electrophilic compound or a dietary cytoprotective compound, Nrf2 is released from the anchor protein Kelch-like ECH-related protein-1 (Keap1) in the cytoplasm and migrates to the nucleus.²⁰ Translocated Nrf2 induces the transcriptional control of the antioxidant response element (ARE) in the promoter region of a target gene, resulting in expression of phase II detoxifying enzymes such as NAD(P)H:quinine oxidoreductase-1 (NQO1) and antioxidation enzymes such as heme oxygenase 1 (HO-1).²¹ Therefore, dietary phytochemicals having effects on Nrf2 activation could be fundamental antioxidant that enhance cellular antioxidant capacity by inducing the gene expression of phase II antioxidant and detoxification enzymes via the Nrf2 pathway.²² Many studies on the anti-inflammatory and anti-carcinogenic effects of various dietary phytochemicals that activate Nrf2 have been published.²³ In the same context, dietary phytochemicals which can activate Nrf2 should be investigated to check the possibility to prevent adipogenesis and lipogenesis.

Neohesperidin found in citrus fruits is flavanone glycoside and has a strong bitter flavor. Citrus flavonoids are the main effective ingredients of citrus species including oranges, tangerines, and lemons. Previous studies revealed that citrus flavonoids have

various pharmacological effects including anti-inflammation, anti-cancer, and cardiovascular protection activities.²⁴ Neohesperidin as one of strong antioxidant has a significant free radical scavenging activity and anti-inflammatory activity as well.²⁵ Furno *et al.* reported that *Citrus bergamia* extract decreased adipogenesis and increased lipolysis.²⁶ *Citrus bergamia* extract is not a pure compound, consisting of naringin, hesperidin, neohesperidin, and neoeriocitrin. After simple hydrogenation, neohesperidin becomes neohesperidin dihydrochalcone (NHDC). There is lack of studies to elucidate that NHDC can suppress adipogenic differentiation and inhibit obesity development.

Thus, in current study, we would like to examine the inhibiting effects of NHDC and other structurally related derivatives on the *in vitro* differentiation of hASC into adipocytes.

1. Hypothesis

From the previous research studies, NHDC have various antioxidant activities. Recent report has shown that citrus extract containing neohesperidin decreased adipogenesis and increased lipolysis. Thus, we can erect a hypothesis that NHDC and structurally related derivatives have anti-adipogenic effect on hASC.

2. Objectives

The main objective of this study is to determine the inhibitory effects of NHDC and its derivatives on *in vitro* adipogenic differentiation of hASC.

3. Scopes of our study

To do this, we are going to evaluate as followings *in vitro* 1) inhibitory activity on adipogenic differentiation of NHDC, 2) anti-oxidative activity of NHDC, 3) anti-adipogenic mechanism of NHDC. Schematic experimental procedures are shown in Fig. 1.

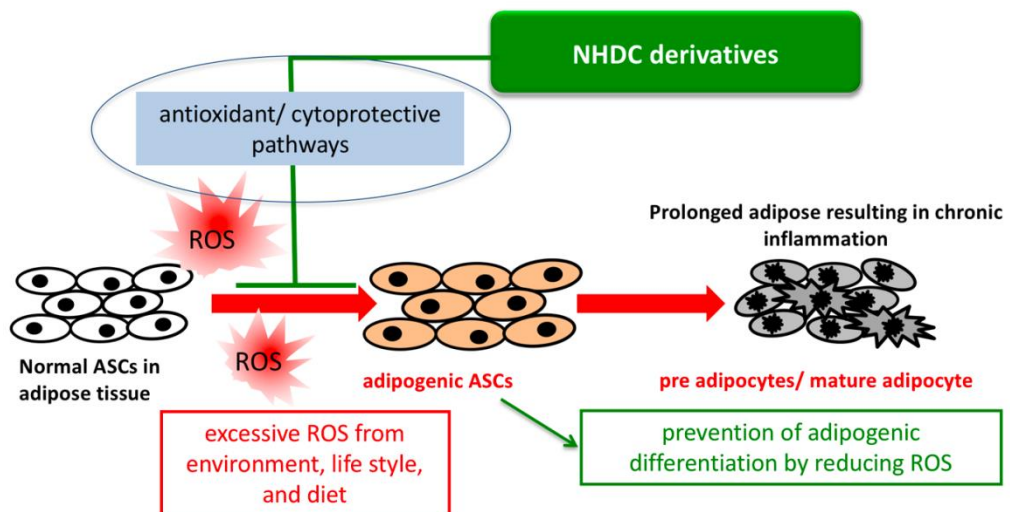


Figure 1. Preventive effects of NHDC derivatives on adipogenic differentiation of hASCs

II. MATERIALS AND METHODS

1. Chemicals and reagents

Dulbecco's modified Eagle's medium (DMEM) and fetal bovine serum (FBS) were obtained from Corning (Acton, MA). The NHDC and its derivatives were kindly provided by professor Suk-Ho Kim, department of Pharmacy, CHA university. Primary antibodies against Actin (sc-1616); Nrf2 (se-722); HO-1 (sc-10789); NQO-1 (sc-32793); PPAR- γ (sc-7196); C/EBP- α (sc-9315) were purchased from Santa Cruz Biotechnology (Santa Cruz, CA). For secondary antibodies, donkey anti-goat immunoglobulin G (IgG)-horseradish peroxidase (HRP) (GTX232040-01) was purchased from GeneTex (Insight Biotech, Wembley, UK), goat anti-rabbit IgG-HRP (sc-2301) was from Santa Cruz Biotechnology, and goat anti-mouse - IgG-HRP conjugates (W 402B) was purchased from Promega (Madison, WI).

2. Cell culture

hASCs obtained from Invitrogen (R7788110) and cultured according to manufacturers' instructions. hASCs were cultured in MesenPRO RSTM Medium (Invitrogen, Carlsbad, CA) supplemented with growth factor and 2mM of L-glutamine and grown at 37°C in a 5% CO₂ humidified atmosphere. The culture

medium was changed every 3 days and the cells were used in early passages (fourth to seventh). Cells were grown up to 70-80% confluence, rinsed with 1X phosphate buffered saline (PBS) (Dyne BIO, Seongnam, Korea) and detached using 0.25% trypsin-EDTA (Gibco, Paisley, Scotland).

3. Synthesis of neohesperidin dihydrochalcone (NHDC) derivatives

Compound **6**, **7**, **8**, **9**, **10**, **11**, **12**, **13** was obtained by condensation with commercially available substituted-benzaldehyde. Benzaldehyde with free hydroxyl group was protected with tetrahydropyran (THP) group (for compound **1**, **2**, **3**, **4**, **5**, **14**). 2,4,6-Trimethoxyacetophenone was synthesized by methylation of 2,4,6-Trihydroxyacetophenone with MeI, K₂CO₃, acetone reflux condition. Spectral data was in agreement with reported data. Chalcone was obtained by aldol condensation of 2,4,6-trimethoxyacetophenone with substituted benzaldehyde.

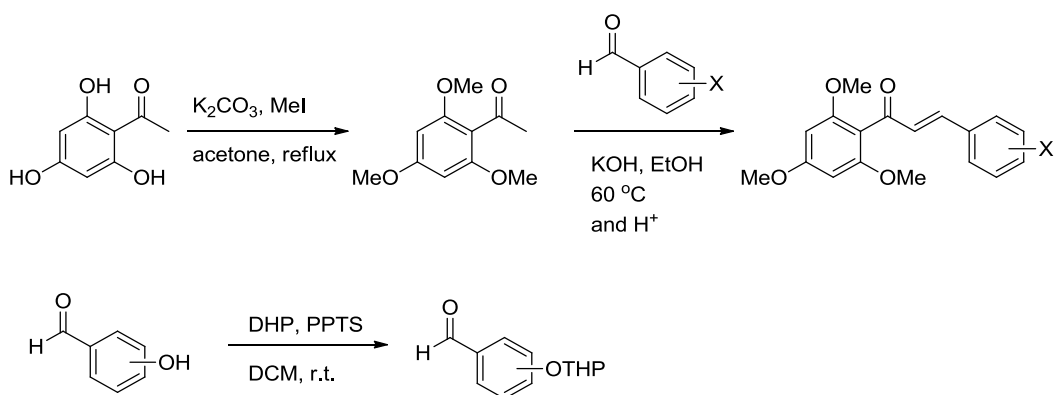


Figure 2. Synthetic scheme of NHDC derivatives

4. Cell viability of hASCs with NHDC derivatives

The cytotoxicity of NHDC and its derivatives on hASCs was estimated using the CellTiter 96 aqueous nonradioactive cell proliferation assay reagent (3-(4,5-dimethylthiazol-2-yl)-5-(3-carboxymethoxyphenyl)-2-(4-sulfophenyl)-2H-tetrazolium, inner salt; MTS) (Promega, Madison, WI). hASCs at a density of 1×10^4 cells/well were cultured in the presence or absence of NHDC and its derivatives at the concentration of 5, 10, 20, 40 $\mu\text{mol/L}$ in the 96-well culture plates. Various concentrations of NHDC and its derivatives were treated on the first and third days. After 5 days, the cell medium was replaced with 15 μl MTS reagent in 100 μl Basal medium and incubated at 37°C with 5% CO_2 for 2h. The absorbance at 490 nm was measured using a microplate reader (Bio-Tek Instruments, Winooski, VT).

5. *In vitro* adipogenic differentiation of hASCs and NHDC derivatives treatment

To investigate the effect of NHDC and derivatives on adipogenic differentiation, differentiation of hASCs into adipocytes was induced. hASCs were seeded at a cell density of 4.0×10^5 cells/well in the proliferation medium (as previously described, MesenPRO RSTM Medium supplemented with growth factor and 2mM of L-glutamine) for 5 days, and treated with adipogenic differentiation medium composed of DMEM-

high glucose (Gibco, Paisley, Scotland), 10% fetal bovine serum (FBS; Gibco, Paisley, Scotland), 1% penicillin-streptomycin (Pen-strep; Gibco, Grand Island, NY), 10 $\mu\text{g/ml}$ insulin (Gibco, Paisley, Scotland), 500 μM isobutyl-methylxanthine (IBMX; Santa Cruz Biotechnology, CA, USA), 200 μM indomethacin (Tokyo Chemical Industry Co., Ltd, Tokyo, Japan), and 1 μM dexamethasone (Sigma-Aldrich, MO) for another 14 days. 4 $\mu\text{mol/L}$ of NHDC and derivatives were treated with differentiation medium as needed. Each proliferation and differentiation medium was changed every three days. The cell morphology was observed and photographed under an inverted fluorescence microscope (Olympus CKX53, Tokyo, Japan). hASCs were cultured in proliferation and differentiation medium in the presence or absence of 4 $\mu\text{mol/L}$ of NHDC or derivatives, and experimental groups are as follows:

Control group (con): No NHDC nor derivative treatment during proliferation media treatment only

Differentiation group (diff): No NHDC nor derivative treatment during proliferation and differentiation media treatment

Sample group (sample number): NHDC or derivative treatment during proliferation and differentiation media treatment

6. Measurement of lipid accumulation during adipogenic differentiation of hASCs with/without NHDC and its derivatives

The accumulation of intracellular lipid droplets was evaluated using Oil Red O (Sigma-Aldrich, MO, USA) staining. The cultured cells were rinsed with PBS and fixed with 4% paraformaldehyde for 15 min at room temperature. After fixation, cells were treated with 60% 2-propanol solution for 10 min. Oil Red O stock solution (0.05% Oil Red O powder in 2-propanol) was diluted with distilled water (volume ratio = 3:2) and filtered through a 0.45 μ M syringe filter. Cells were incubated with diluted Oil Red O solution for 30 min at room temperature. After that, the stained cells were washed with PBS three times to remove background. To evaluate the degree of adipogenic differentiation, the photomicrographs of the stained cells were captured by optical microscopy. For quantification of Oil Red O uptake by the lipids, the dye was eluted with 100% 2-propanol and measured at an absorbance of 510 nm with ELISA reader (Bio-Tek Instruments, Winooski, VT).

7. Reactive oxygen species (ROS) measurement

The intracellular ROS level was assessed using 2',7'-dichlorofluorescein diacetate (H_2DCFDA) (D399; Invitrogen, Carlsbad, CA). H_2DCFDA is deacetylated intracellularly by esterase, forming H_2DCF , which is oxidized by ROS to 2',7'-dichlorofluorescein (DCF), a highly fluorescent compound. Cells were plated at a seeding density of 2.5×10^5 cells/well in a 60 mm culture plate and proceeded adipogenic differentiation with or without 4 μ mol/L of NHDC and derivatives. On 14th days, cells were washed with the PBS and harvested using trypsin-EDTA. After

the harvest cells were resuspended and incubated in pre-warmed PBS containing 10 μ M DCFDA for 30 min at 37°C. Then it was transferred to 5 ml FACS tube (SPL Life Science, Pocheon, Korea). Intracellular fluorescence was then quantified using a BD Calibur flow cytometer (Becton Dickinson, NJ) at excitation wavelength of 488 nm and at emission wavelength of 530 nm. Data analyses were based on 10,000 detected events using the Cell Quest software.

8. Quantitative reverse transcription-polymerase chain reaction (qRT-PCR) analysis

The cell pellet was obtained after being differentiated for 14 days. Total RNA from hASC were purified by Rneasy Mini Kit (Qiagen, Gaithersburg, MD) according to manufacturer's protocol. cDNA was synthesized from 1 μ g of total RNA by reverse transcription using dNTP mix, Rnase inhibitor (Enzynomics Co., Ltd., Daejeon, Korea), M-MLV Reverse Transcriptase, M-MLV RT 5X Buffer (Promega Corporation, Madison, WI, USA) and random oligo primers. qRT-PCR was performed using SYBR Green 2x Mastermix kit (Messeger of biotechnology, Hanam, Korea) on a BioRad CFX96 Real-Time PCR Detection System instrument (Bio-Rad Laboratories, Hercules, CA) under the following conditions: 95°C for 10 min followed by 40 cycles of 15 s of denaturation at 95°C and 60 s of annealing and elongation at 60°C. A melting curve analysis was performed after each run to confirm product specificity. The delta-delta-Ct method was employed to determine the relative

gene expression level of gene of interest normalized to the house-keeping gene Glyceraldehyde-3-phosphate dehydrogenase (GAPDH). The following primer sequences were used : GAPDH (forward: 5'- AAG GGT CAT CAT CTC TGC CC-3' and reverse: 5'-ATG ATG TTC TGG AGA GCC CC-3'), Nrf2 (forward: 5'-TCC TCT CCA CAG AAG ACC CC-3' and reverse: 5'-TCA GGG TGG TTT TGG TTG AA-3'), HO-1 (forward: 5'-ACA TCT ATG TGG CCC TGG AG-3' and reverse: 5'-TGT TGG GGA AGG TGA AGA AG-3'), NQO-1 (forward: 5'-CAC ACT CCA GCA GAC GCC CG-3' and reverse: 5'-TGC CCA AGT CAT GGC CCA CAG-3'), and PPAR- γ (forward: 5'-TCT CTC CGT AAT GGA AGA CC-3' and reverse: 5'-GCA TTA TGA GAC ATC CCC AC-3').

9. Western blot analysis

Cells were washed twice with ice-cold PBS, lysed with 300 μ L of RIPA buffer (Sigma-Aldrich, MO), and centrifuged at 14,000 rpm for 10 min (to clarify lysates). Approximately 30 μ g of total protein was separated by SDS-polyacrylamide gel electrophoresis (PAGE). Proteins were transferred to polyvinylidene fluoride membranes (PVDF) using the trans-Blot semi-dry transfer kit (Bio-Rad, Hercules, CA), blocked for 1 h with 5% nonfat dry milk in Tris-buffered saline (TBS) with 0.1% Tween-20 (TBS-T), solution for 1-16 h. Membranes were washed several times in TBS-T solution and incubated with HRP-conjugated secondary antibodies (0.1 mg/mL; Jackson Immunoresearch Laboratories). Immunoreactivity was detected

using the WEST-one western blotting detection system (iNtRON Biotechnology, Seoul, Korea).

10. Statistic analysis

Data are presented as mean \pm standard deviation (SD) or standard error (SE). Data are compared using Student's t-test. All analyses are conducted using SAS statistical software, version 9.1 (SAS Institute Inc, Cary, NC, USA). All statistical tests are two-sided and statistical significance is determined at a p -value < 0.05 .

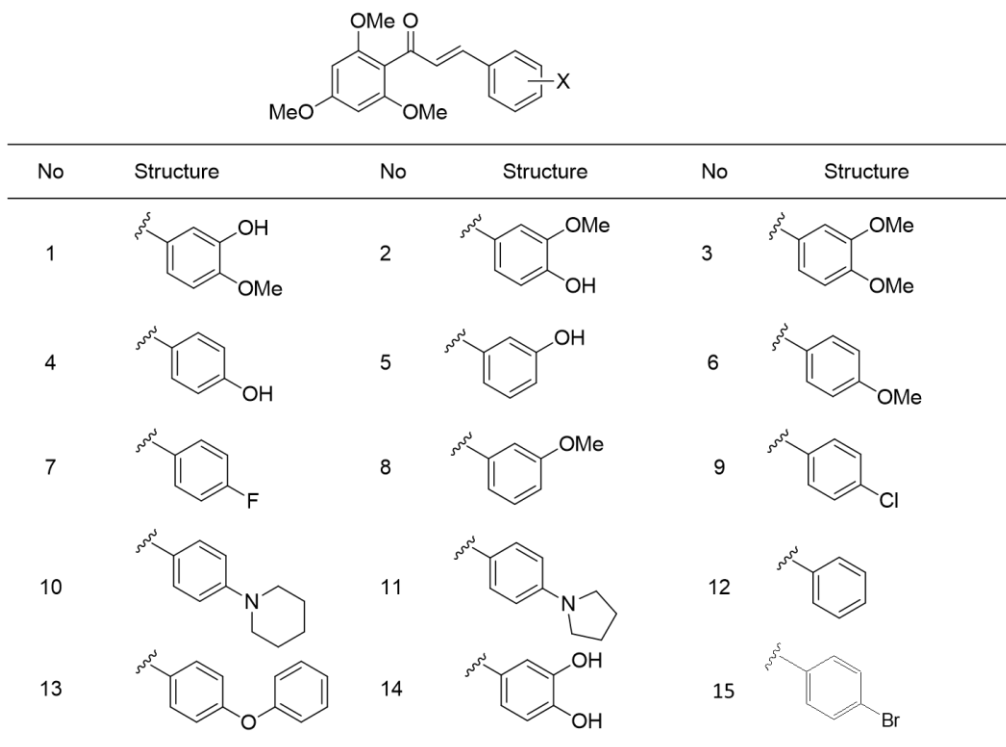
III. RESULTS

1. Chemistry

Unless noted otherwise, all starting materials and reagents were obtained commercially and were used without further purification. Tetrahydrofuran was distilled from sodium benzophenoneketyl. Dichloromethane and acetonitrile were freshly distilled from calcium hydride. All solvents used for routine product isolation and chromatography were of reagent grade and glass distilled. Reaction flasks were dried at 100°C before use, and air and moisture sensitive reactions were performed under nitrogen. Flash column chromatography was performed using silica gel 60

(230–400 mesh, Merck, Kenilworth, NJ) with the indicated solvents. Thin-layer chromatography was performed using 0.25 mm silica gel plates (Merck). Mass spectra were obtained using a VG Trio-2 GC-MS instrument, and high resolution mass spectra were obtained using a JEOL JMS-AX 505WA unit. ^1H and ^{13}C spectra were recorded on a JEOL JNM-LA 300, Bruker Analytik ADVANCE digital 400, ADVANCE digital 500 or JEOL ECA-600 spectrometer in deuteriochloroform (CDCl_3) or deuteriomethanol (CD_3OD). Chemical shifts are expressed in parts per million (ppm, δ) downfield from tetramethylsilane and are referenced to the deuterated solvent (CHCl_3). ^1H -NMR data are reported in the order; chemical shift, multiplicity (s, singlet; bs, broad singlet; d, doublet; t, triplet; q, quartet; m, multiplet, and/or multiple resonance, numbers of protons, and coupling constants in hertz (Hz). All the final compounds were purified up to more than 95% purity. The purities were determined by a reverse-phase high-performance liquid chromatography (Waters, Milford, MA., 254 nm) using Eclipse Plus C18 (4.6 x 250mm) with an isocratic flow ($\text{MeOH} : \text{H}_2\text{O} = 9 : 1$) at 1.5 mL/min.

In this research, the compound number was used instead of the synthesized derivative name (Fig. 3).

Figure 3. Structures of synthesized NHDC and its derivatives


1.1 (*E*)-3-(3-hydroxy-4-methoxyphenyl)-1-(2,4,6-trimethoxyphenyl)prop-2-en-1-one

Yellow solid; m.p. 196 – 198 °C; ¹H-NMR (CDCl₃, 300MHz) δ 7.26 (d, 1H, *J* = 16.0 Hz), 7.12 (d, 1H, *J* = 2.1 Hz), 7.00 (dd, 1H, *J* = 8.4, 2.1 Hz), 6.81 (d, 1H, *J* = 16.0 Hz), 6.80 (d, 1H, *J* = 8.4 Hz), 6.13 (s, 2H), 5.62 (s, 1H), 3.89 (s, 3H), 3.83 (s, 3H), 3.74 (s, 6H); HRMS (ESI) Calculated for C₁₉H₂₀O₆ ([M]⁺): 344.1260, C₁₉H₂₁O₆ ([M + H]⁺): 345.1338 found: 169.1020.

1.2 (*E*)-3-(4-hydroxy-3-methoxyphenyl)-1-(2,4,6-trimethoxyphenyl)prop-2-en-1-one

Yellow solid; m.p. 128 – 130 °C; ¹H-NMR (CDCl₃, 300MHz) δ 7.27 (d, 1H, *J* = 15.9 Hz), 7.06 – 7.02 (m, 2H), 6.89 (d, 1H, *J* = 8.6 Hz), 6.83 (d, 2H, *J* = 15.9 Hz), 6.16 (s, 2H), 5.96 (s, 1H), 3.90 (s, 3H), 3.86 (s, 3H), 3.76 (s, 6H); HRMS (ESI) Calculated for C₁₉H₂₀O₆ ([M]⁺): 344.1260, C₁₉H₂₁O₆ ([M +H]⁺): 345.1338 found: 169.1020.

1.3 (*E*)-3-(3,4-dimethoxyphenyl)-1-(2,4,6-trimethoxyphenyl)prop-2-en-1-one

Yellow solid; m.p. 238 – 240 °C; ¹H-NMR (CDCl₃, 300MHz) δ 7.26 (d, 1H, *J* = 15.9 Hz), 7.08-7.04 (m, 2H), 6.84-6.79 (m, 2H), 6.14 (s, 2H), 3.87 (s, 3H), 3.84 (s, 3H), 3.75 (s, 6H); HRMS (ESI) Calculated for C₂₀H₂₂O₆ ([M]⁺): 358.1416, C₂₀H₂₃O₆ ([M +H]⁺): 359.1495 found: 169.1020.

1.4 (*E*)-3-(4-hydroxyphenyl)-1-(2,4,6-trimethoxyphenyl)prop-2-en-1-one

Yellow solid; m.p. 184 – 186 °C; ¹H-NMR (CDCl₃, 300MHz) δ 7.40 (d, 2H, *J* = 8.6 Hz), 7.28 (d, 1H, *J* = 15.9 Hz), 6.82 (d, 1H, *J* = 15.9 Hz), 6.80 (d, 2H, *J* = 8.6 Hz), 6.13 (s, 2H), 5.45 (s, 1H), 3.84 (s, 3H), 3.74 (s, 6H); HRMS (ESI) Calculated for C₁₈H₁₈O₅ ([M]⁺): 314.1154, C₁₈H₁₉O₅ ([M +H]⁺): 315.1232, found: 169.1020.

1.5 (*E*)-3-(3-hydroxyphenyl)-1-(2,4,6-trimethoxyphenyl)prop-2-en-1-one

Yellow solid; m.p. 206 – 207 °C; ¹H-NMR (CD₃OD, 300MHz) δ 7.90 (s, 2H), 7.22 (d, 1H, *J* = 15.9 Hz), 7.20 (t, 1H, *J* = 7.9 Hz), 7.00 (d, 1H, *J* = 7.9 Hz), 6.95 (t, 1H, *J* = 2.0 Hz), 6.86 (td, 1H, *J* = 15.9 Hz), 6.82 (m, 1H), 6.28 (s, 2H), 3.86 (s, 3H), 3.76 (s, 6H); HRMS (ESI) Calculated for C₁₈H₁₈O₅ ([M]⁺): 314.1154, C₁₈H₁₉O₅ ([M +H]⁺): 315.1232found: 169.1020.

1.6 (*E*)-3-(4-methoxyphenyl)-1-(2,4,6-trimethoxyphenyl)prop-2-en-1-one

Yellow oil; ¹H-NMR (CDCl₃, 300MHz) δ 7.43 (dt, 2H, *J* = 8.7, 2.8 Hz), 7.27 (d, 1H, *J* = 16.0 Hz), 6.83 (dt, 2H, *J* = 8.7, 2.8 Hz), 6.80 (d, 1H, *J* = 16.0 Hz), 6.11 (s, 2H), 3.81 (s, 3H), 3.78 (s, 3H), 3.71 (s, 6H); HRMS (ESI) Calculated for C₁₉H₂₀O₅ ([M]⁺): 328.1311, C₁₉H₂₁O₅ ([M +H]⁺): 329.1389, found: 169.1020.

1.7 (*E*)-3-(4-fluorophenyl)-1-(2,4,6-trimethoxyphenyl)prop-2-en-1-one

Yellow oil; ¹H-NMR (CDCl₃, 300MHz) δ 7.53 – 7.44 (m, 2H), 7.31 (d, 1H, *J* = 15.9 Hz), 7.06 – 7.02 (m, 2H), 6.86 (d, 1H, *J* = 15.9 Hz), 6.13 (s, 2H), 3.83 (s, 3H), 3.74 (s, 6H); HRMS (ESI) Calculated for C₁₈H₁₇FO₄ ([M]⁺): 316.1111, C₁₈H₁₈FO₄ ([M +H]⁺): 317.1189, found: 169.1020.

1.8 (E)-3-(3-methoxyphenyl)-1-(2,4,6-trimethoxyphenyl)prop-2-en-1-one

Yellow oil; $^1\text{H-NMR}$ (CDCl_3 , 300MHz) δ 7.31 (d, 1H, $J = 16.1$ Hz), 7.26 (t, 1H, $J = 8.0$ Hz), 7.09 (d, 1H, $J = 8.0$ Hz), 7.02 (t, 1H, $J = 1.9$ Hz), 6.92 (d, 1H, $J = 16.1$ Hz), 6.89 (ddd, 2H, $J = 8.0, 2.5, 0.8$ Hz), 6.14 (s, 2H), 3.84 (s, 3H), 3.79 (s, 3H), 3.73 (s, 6H); HRMS (ESI) Calculated for $\text{C}_{19}\text{H}_{20}\text{O}_5$ ($[\text{M}]^+$): 328.1311, $\text{C}_{19}\text{H}_{21}\text{O}_5$ ($[\text{M} + \text{H}]^+$): 329.1389, found: 169.1020.

1.9 (E)-3-(4-chlorophenyl)-1-(2,4,6-trimethoxyphenyl)prop-2-en-1-one

Yellow solid; m.p. 124 – 126 °C; $^1\text{H-NMR}$ (CDCl_3 , 300MHz) δ 7.44 (d, 2H, $J = 8.6$ Hz), 7.31 (d, 2H, $J = 8.6$ Hz), 7.33 – 7.27 (m, 3H), 6.90 (d, 1H, $J = 15.9$ Hz), 6.13 (s, 2H), 3.84 (s, 3H), 3.75 (s, 6H); HRMS (ESI) Calculated for $\text{C}_{18}\text{H}_{17}\text{ClO}_4$ ($[\text{M}]^+$): 332.0815, $\text{C}_{18}\text{H}_{18}\text{ClO}_4$ ($[\text{M} + \text{H}]^+$): 333.0894, found: 169.1020.

1.10 (E)-3-(4-(piperidin-1-yl)phenyl)-1-(2,4,6-trimethoxyphenyl)prop-2-en-1-one

Yellow solid; m.p. 118 – 120 °C; $^1\text{H-NMR}$ (CDCl_3 , 300MHz) δ 7.37 (d, 2H, $J = 9.3$ Hz), 7.23 (d, 1H, $J = 15.9$ Hz), 6.81 (d, 2H, $J = 9.3$ Hz), 6.76 (d, 1H, $J = 15.9$ Hz), 6.13 (s, 2H), 3.82 (s, 3H), 3.72 (s, 6H); 333.0894; HRMS (ESI) Calculated for $\text{C}_{23}\text{H}_{27}\text{NO}_4$ ($[\text{M}]^+$): 381.1940, $\text{C}_{23}\text{H}_{28}\text{NO}_4$ ($[\text{M} + \text{H}]^+$): 382.2018, found: 169.1020.

1.11 (*E*)-3-(4-(pyrrolidin-1-yl)phenyl)-1-(2,4,6-trimethoxyphenyl)prop-2-en-1-one

Yellow solid; m.p. 166 – 167 °C; ¹H-NMR (CDCl₃, 300MHz) δ 7.37 (d, 2H, *J* = 8.8 Hz), 7.24 (d, 1H, *J* = 15.8 Hz), 6.74 (d, 1H, *J* = 15.8 Hz), 6.47 (d, 2H, *J* = 8.8 Hz), 6.13 (s, 2H), 3.83 (s, 3H), 3.73 (s, 6H), 3.30 (m, 4H), 1.99 (m, 4H); HRMS (ESI) Calculated for C₂₂H₂₅NO₄ ([M]⁺): 367.1784, C₂₂H₂₆NO₄ ([M +H]⁺): 368.1862, found: 169.1020.

1.12 (*E*)-3-phenyl-1-(2,4,6-trimethoxyphenyl)prop-2-en-1-one

Yellow oil; ¹H-NMR (CDCl₃, 300MHz) δ 7.52 – 7.45 (m, 2H), 7.37 – (m, 4H), 6.94 (d, 1H, *J* = 15.9 Hz), 6.14 (s, 2H), 3.84 (s, 3H), 3.75 (s, 6H); HRMS (ESI) Calculated for C₁₈H₁₉O₄ ([M]⁺): 298.1205, C₁₈H₂₀O₄ ([M +H]⁺): 299.1283, found: 169.1020.

1.13 (*E*)-3-(4-phenoxyphenyl)-1-(2,4,6-trimethoxyphenyl)prop-2-en-1-one

Yellow oil; ¹H-NMR (CDCl₃, 300MHz) δ 7.47 (d, 2H, *J* = 4.4 Hz), 7.38 – 7.29 (m, 3H), 7.13 (t, 1H, *J* = 7.4 Hz), 7.03 – 6.98 (m, 2H), 6.94 (t, 2H, *J* = 4.4 Hz), 6.85 (d, 1H, *J* = 15.9 Hz), 6.14 (s, 2H), 3.83 (s, 3H), 3.75 (s, 6H); HRMS (ESI) Calculated for C₂₄H₂₂O₅ ([M]⁺): 390.1467, C₂₄H₂₃O₅ ([M +H]⁺): 391.1545, found: 169.1020.

1.14 (*E*)-3-(3,4-dihydroxyphenyl)-1-(2,4,6-trimethoxyphenyl)prop-2-en-1-one

Yellow solid; m.p. 177 – 178 °C; ¹H-NMR (acetone-d₆, 300MHz) δ 8.37 (bs, 1H), 7.13 (d, 1H, *J* = 16.0 Hz), 7.12 (d, 1H, *J* = 2.0 Hz), 6.96 (dd, 1H, *J* = 8.1, 2.0 Hz), 6.83 (d, 1H, *J* = 8.1 Hz), 6.68 (d, 1H, *J* = 16.0 Hz), 6.28 (s, 2H), 3.85 (s, 3H), 3.73 (s, 6H); HRMS (ESI) Calculated for C₁₈H₁₈O₆ ([M]⁺): 330.1103, C₁₈H₁₉O₆ ([M +H]⁺): 331.1182, found: 169.1020.

1.15 (*E*)-3-(4-bromophenyl)-1-(2,4,6-trimethoxyphenyl)prop-2-en-1-one

Yellow solid; m.p. 112 – 114 °C; ¹H-NMR (CDCl₃, 300MHz) δ 7.45 (dt, 2H, *J* = 8.5, 2.0 Hz), 7.34 (dt, 2H, *J* = 8.5, 2.0 Hz), 7.27 (d, 1H, *J* = 16.1 Hz), 6.90 (d, 1H, *J* = 16.1 Hz), 6.11 (s, 2H), 3.81 (s, 3H), 3.73 (s, 6H); HRMS (ESI) Calculated for C₁₈H₁₇BrO₄ ([M]⁺): 376.0310, C₁₈H₁₈BrO₄ ([M +H]⁺): 377.0388, found: 169.1020.

2. Cell viability of hASCs by NHDC and derivatives treatment

hASCs were seeded at a density of 1×10⁴ cells/well on 96 well plate culture plates and then grown in 0, 5, 10, 20, or 40 μM of NHDC and derivatives for 5 days. Figure 4 shows the cytotoxicity of NHDC and its derivatives. The viability of hASCs was measured against total of 16 compounds including NHDC, and calculated as a percentage of the untreated control. Most of the compounds showed little cytotoxicity up to a concentration of 20 μM. However, some compounds start to show cytotoxicity

when the concentration reaches 40 μM . In particular, compounds 7, 9, and 12 lowered the viability of hASC to 80% at a concentration of 40 μM . Compound 7 lowered the survival rate of hASC to lesser than 60% even at 5 μM . Therefore, we determined the treatment concentration of the compound by 4 μM . The inhibition of adipogenic differentiation of hASC was tested against compounds 9, and 12, which exhibit cytotoxicity at high concentration along with NHDC.

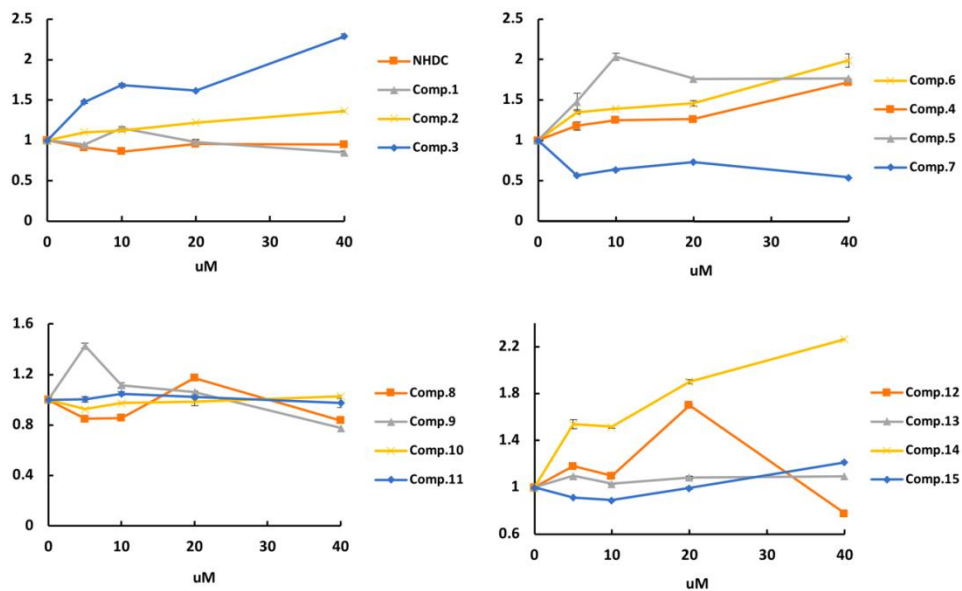


Figure 4. Viability of human adipose-derived stem cells (hASC) in the presence of NHDC and its derivatives. Human adipose-derived stem cells (hASCs) were seeded onto a 96-well plate, and the cells were treated with different concentrations (5, 10, 20, and 40 μM) of NHDC and its derivatives for 5 days. The cell viability was measured by MTS assay. The results are expressed as the mean values \pm S.D (n = 3).

3. Inhibition effects of NHDC derivatives on the adipogenic differentiation of hASCs

To examine the effect of NHDC and derivatives on adipogenic differentiation, hASCs were differentiated into adipocytes using adipogenic differentiation media and treated with NHDC and derivatives. Induction of hASCs' differentiation into adipocytes was evaluated by Oil Red O staining and quantified by the extraction of Oil Red O from stained cells. In control group, almost no Oil Red O staining was observed. In contrast, differentiation group showed the highest Oil Red O staining among all groups (Fig. 5A). In the NHDC treated group, slightly reduced Oil Red O staining was observed compared with the differentiated group. In addition, the amount of lipid accumulation decreased in the order of compounds 12 and 9. Interestingly, in compound 9 group, which showed the highest decrease in lipid accumulation, the lipid accumulation was decreased by 25% as compared with the differentiated group (Fig. 5B). In addition, the expression of PPAR- γ , the important adipogenic differentiation marker, was measured in protein level. The expression of PPAR- γ in compound 9 and 12 treated groups was decreased by 46.7% and 70% respectively, compared to adipogenic differentiation group. (Fig. 5C, D). Then, quantitative-PCR was also performed to measure the PPAR- γ mRNA expression to see the gene level effect. The results showed that the derivatives reduced the expression of PPAR- γ mRNA compared to differentiation group, which is in concordance with the Oil Red O staining analysis (Fig 5E). These results indicate that NHDC derivatives can inhibit the adipogenic differentiation of hASCs through down-regulating PPAR- γ .

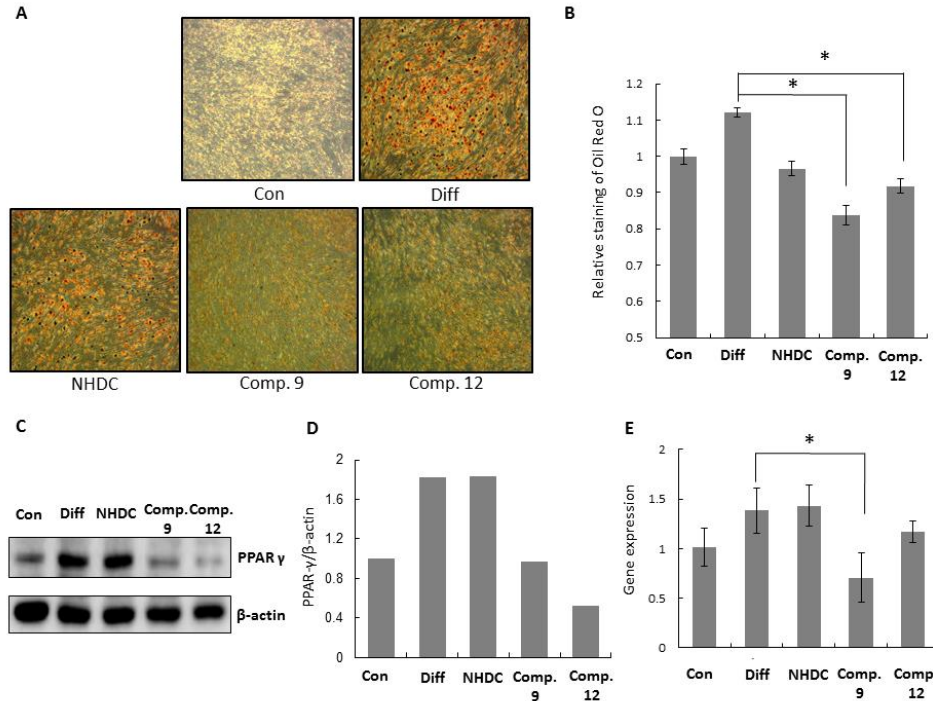


Figure 5. Effect of NHDC and its derivatives on adipogenic differentiation. Cells were seeded on 12-well plate and cultured for 14 days with or without differentiation medium and compounds. Differentiated hASCs were stained with Oil Red O at day 15 as described in Materials and Methods (A). Lipid accumulation was quantified by Oil Red O uptake and the amount of eluted dye was measured at the absorbance of 510 nm (B). Through Western Blotting assay of PPAR- γ and its quantification, Bands' densities were analyzed by using ImageJ software (<http://rsbweb.nih.gov/ij>) (D). Quantitative RT-PCR results of PPAR- γ were checked (E). The results are expressed as the mean values \pm S.D (n = 3); * $P < 0.01$ as compared to the differentiation group. Con, control group cultured in growth medium only; Diff, differentiation group cultured in adipogenic differentiation medium.

4. Anti-lipogenesis effect of NHDC derivatives during adipogenic differentiation of hASCs

Before observing the anti-lipogenic effects of NHDC derivatives, we investigated changes in the expression of adipogenic differentiation markers over time after the treatment of adipogenic differentiation medium. The expression of adipogenic differentiation marker including PPAR- γ and C/EBP- α and the expression of intracellular lipogenesis markers such as FAS and SREBP-1 were observed at days 6 and 9 after adipogenic differentiation treatment. To see the early stage of adipogenic differentiation, hASCs were harvested at 6 days after adipogenic induction. Meanwhile, late stage of adipogenic differentiation was investigated at 9 days after adipogenic induction. Expression of transcription factor, Nrf2 and its downstream antioxidant enzymes including HO-1 and NQO-1 were observed as well. Both the expression of adipogenic markers and intracellular lipogenesis markers were increasing as the differentiation proceeded. However, the expression of differentiation markers was gradually increased with late stage of differentiation, while the expression of lipogenesis markers showed remarkable increase. Interestingly, the expression of Nrf2 and its downstream antioxidant enzymes such as HO-1 and NQO-1 were decreased as the adipogenic differentiation was proceeded (Fig. 6).

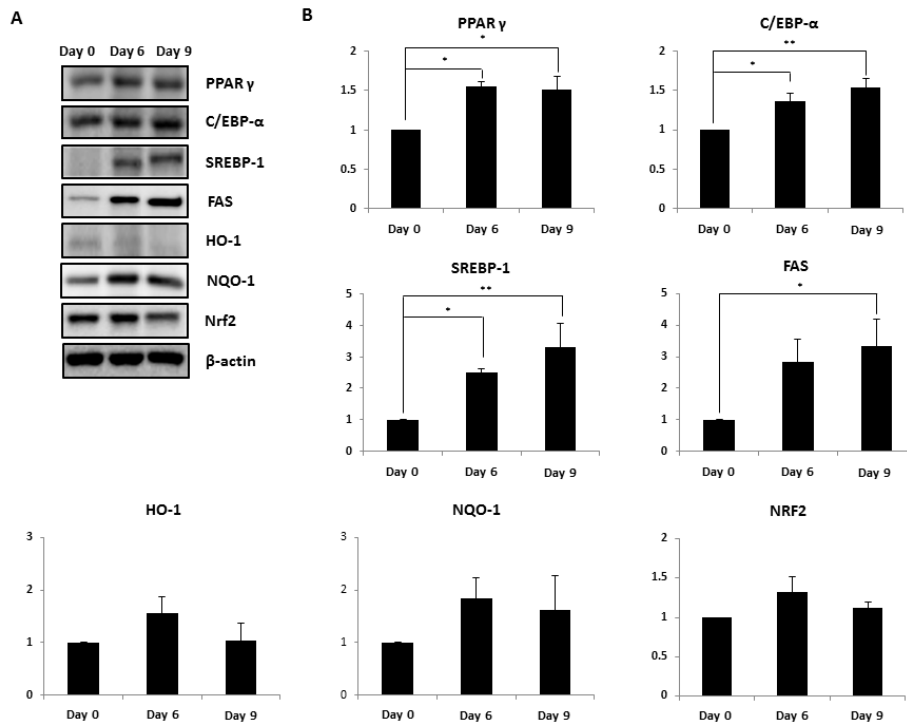


Figure 6. Changes in expression of adipogenic and lipogenic markers over time.

The expression of PPAR- γ , C/EBP- α , FAS, SREBP-1, NQO-1, HO-1, and Nrf2 were measured by Western Blotting at two-time points. To see the early stage of adipogenic differentiation, hASCs were harvested at 6 days after adipogenic induction. Meanwhile, late stage of adipogenic differentiation was investigated at 9 days after adipogenic induction (A). Bands were densitometric analyzed by using ImageJ software (<http://rsbweb.nih.gov/ij>) (B). The results are expressed as the mean values \pm S.D (n = 3); * P < 0.01, ** P < 0.05 as compared to the control group. Day 0, hASCs were cultured in growth medium only; Day 6 and Day 9, hASCs were cultured in adipogenic differentiation medium for 6 or 9 days respectively.

To confirm the effect of NHDC derivatives on adipogenesis at late stage of adipogenic differentiation, the protein levels of adipogenic and lipogenic gene products were examined. As shown in Figure 7A, FAS and SREBP-1 expression in differentiated group was up-regulated, but the high level of expression of these adipogenic regulators was decreased by NHDC derivatives not by NHDC. Expression of FAS was decreased by 51.6% and 38.7% by compounds 9 and 12, respectively (Fig. 7B). Additionally, compounds 9 and 12 reduced the expression of SREBP-1, common transcription factor regulating fatty acid synthesis by 65.7% and 60%, respectively (Fig 7C). These data indicated that HNDC derivatives could affect lipogenesis during the hASC differentiation.

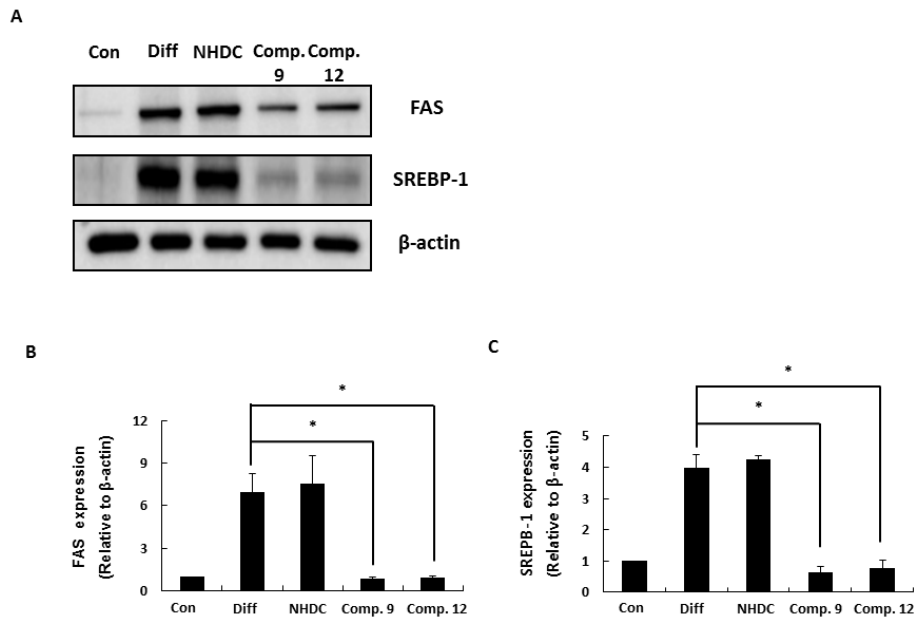


Figure 7. Effect of NHDC derivatives on lipogenesis during the adipogenic differentiation. hASCs were treated with NHDC or its derivatives after the induction of adipogenic differentiation for 14 days. Western Blotting was performed against lipogenic markers including FAS and SREBP-1 (A). Densitometric analysis of Western Blotting of FAS (B) and SREBP-1 (C). Bands were densitometric analyzed by using ImageJ software. The results are expressed as the mean values \pm S.D (n = 3); *P < 0.01 as compared to the control group. Con, control group cultured in growth medium only; Diff, differentiation group cultured in adipogenic differentiation medium.

5. Effect of NHDC and derivatives on ROS generation during adipogenic differentiation of hASCs

To measure the intracellular ROS level in differentiated hASCs, ROS in cells were stained with H₂DCFDA. Once the staining agent, the acetate ester form of H₂DCFDA, penetrates the cell membrane, intracellular ROS oxidize DCFDA to DCF, resulting in the generation of fluorescence. The stained cells were applied to flow cytometry and the level of fluorescence was quantified. As shown in Figure 8, differentiation group showed higher intensity of fluorescence level compared with control. Strong fluorescence means that the ROS were present in cells at a high concentration. Therefore, when hASCs differentiated into adipocytes by adipogenic differentiation medium, relatively high concentration of ROS accumulated in the cells (Fig. 8A). Although the fluorescent intensity of experimental groups including NHDC and compound 12 were not dramatically weaker than differentiation group, compound 9 showed strong reduction of fluorescence (Fig. 8B). These data indicated that compound 9 appeared to have strong inhibition effect on ROS generation.

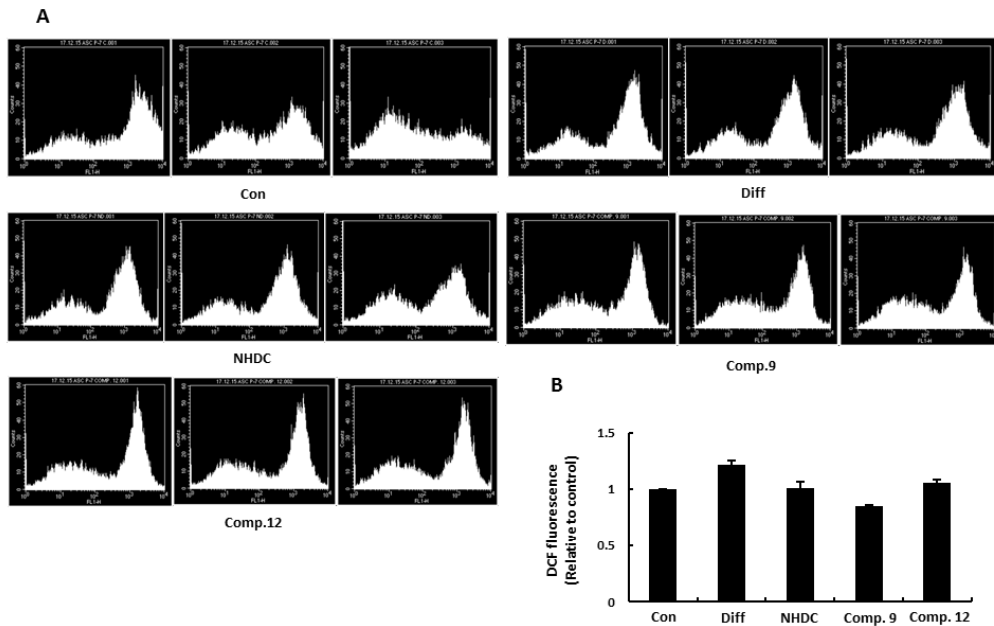


Figure 8. ROS-mediated adipogenic differentiation in hASCs. hASCs were treated with normal growth medium for 5 day and then treated with differentiation medium with NHDC or its derivatives for 14 days. Meanwhile control group were treated with growth medium only for 5 days. Intracellular ROS levels were estimated by flow cytometric analysis of DCF fluorescence after staining cells with DCFH-DA. Flow cytometric distribution of DCFDA stained hASCs. (A). Cell granularity of DCF-fluorescence was evaluated (B). The results are expressed as the mean values \pm S.D (n = 3); Con, control group cultured in growth medium only; Diff, differentiation group cultured in adipogenic differentiation medium.

6. Induction of Nrf2 and its downstream antioxidant enzymes by NHDC and derivatives in adipogenic differentiation of hASCs

In order to elucidate the cause for the reduction of intracellular ROS production in the experimental groups treated with NHDC derivatives, the expression of Nrf2, a regulator of antioxidant enzymes, was investigated (Fig. 9). First, the protein levels of the gene products of Nrf2 and its downstream enzymes were examined by Western blot analysis. Expression of Nrf2 protein did not show any statistically significant difference, but significant increased expression was observed in the group treated with compound 12 compared to the differentiation group (Fig. 9B). Relatively, the expression of HO-1 and NQO-1, the downstream antioxidant enzymes of Nrf2, was significantly increased in the NHDC-treated experimental group (Fig. 9C and D). Then, the effect of NHDC derivatives on the expression of genes associated with antioxidant enzyme was investigated. The expression levels of mRNA of these genes were measured by quantitative PCR. The increase in mRNA levels of Nrf2 and its downstream genes in derivative treated groups were correlated with protein levels of gene products (Fig. 9E to G). These results indicate that NHDC derivatives could inhibit adipogenic differentiation in hASC through the activation of Nrf2 pathway, which is due to regulation of ROS production by upregulating the Nrf2 downstream genes including HO-1 and NQO1.

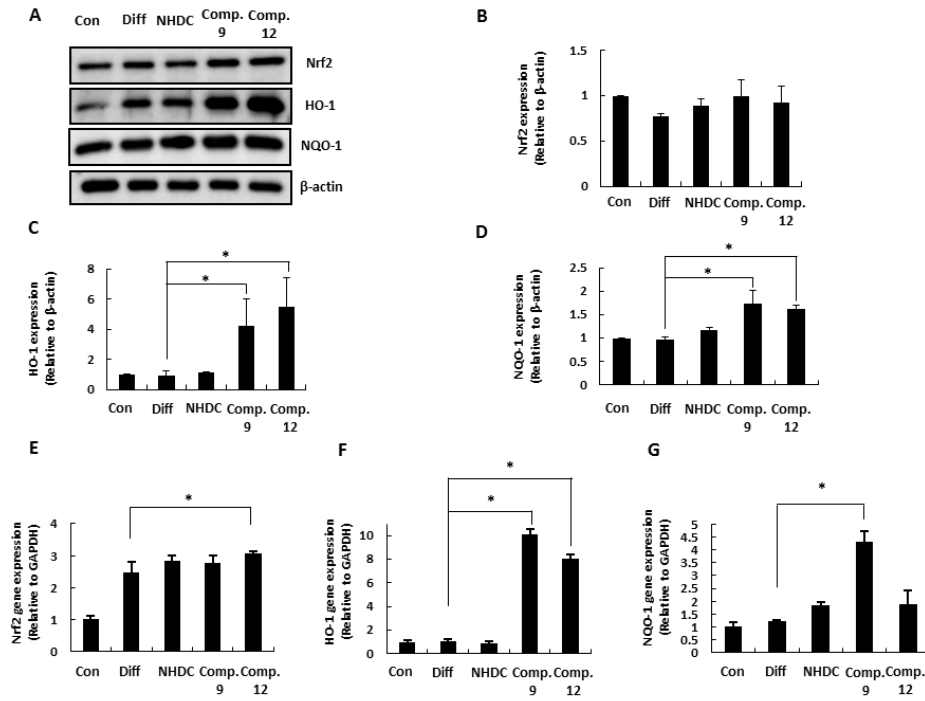


Figure 9. Activation of Nrf2 pathway by NHDC and its derivatives in hASCs. hASCs except control group were treated with differentiation medium and NHDC, compound 9, and compound 12 (4 μ M). The cells were harvested at 14 days after adipogenic induction to examine the expression of Nrf2 and downstream enzymes. Western blotting was performed against Nrf2 and its downstream antioxidant enzymes (A). Quantitative values of the expression of Nrf2, HO-1, and NQO-1 were calculated by normalization with β -actin (B), (C), and (D) respectively. Gene expression levels of Nrf2 and its downstream enzymes using quantitative RT-PCR were evaluated (E), (F), and (G). The results are expressed as the mean \pm S.D (n = 3); * $P < 0.01$ as compared to the differentiation group. Con, control group cultured in

growth medium only; Diff, differentiation group cultured in adipogenic differentiation medium.

IV. DISCUSSION

Recently, much attention had been paid on the worldwide increase of obesity which could be causes of various diseases including cardiovascular and degenerative diseases. Many researchers in the obesity and adipocyte field have focused on therapeutic methods of weight loss, including diet, behavioral and pharmacologic therapy. Unfortunately, to obtain the successful result in dietary and behavioral therapy for obesity, sustained efforts by individuals are required. Also, there is no evidence that pharmacologic therapy is more effective than other therapies.²⁷ Therefore, in order to promote both individual and public health, a new point of view in obesity treatment is necessary. Several reports demonstrated that Nrf2 which is the transcription factor regulating antioxidant enzymes could inhibit adipogenic differentiation in preadipocytes.^{28,29} In addition, MSCs present abundantly in abdomen are able to differentiate into three lineages such as chondrogenic, osteogenic, and adipogenic.⁷ It is known that when adipogenic differentiation occurs, intracellular ROS concentration in MSCs increases.³⁰ From our study, the expression of PPAR- γ and C/EBP- α , an adipocyte differentiation marker, is dominant at the early stage of adipogenic differentiation. As the differentiation progresses, the expression of

lipogenesis markers, such as FAS and SREBP-1, were increased, which was correlated with the decreased expression of Nrf2 (Fig. 6). Therefore, it can be hypothesized that activation of intracellular antioxidant mechanism by Nrf2 may reduce intracellular ROS and inhibit the adipogenic differentiation of hMSC. Neohesperidin as one of strong antioxidants has a significant free radical scavenging activity and anti-inflammatory activity as well.²⁵ After simple hydrogenation, neohesperidin becomes NHDC. Based on the antioxidant potential of neohesperidin and NHDC, 15 novel derivatives were synthesized and utilized to see the anti-adipogenic differentiation effect of these compounds.

In the present study, we investigated whether NHDC and its derivatives could inhibit hASC differentiation into adipocytes by reducing ROS production through Nrf2 pathway. NHDC derivatives reduced the lipid accumulation in differentiated group compared with control, which was measured with Oil Red O staining. In cell viability test, compound 9 and 12 showed 20% cell death at 40 μ M concentration, but cell death was not affected by Oil Red O staining because the concentration applied in this experiment was 4 μ M which has no cytotoxic effect. As mentioned above, the cell viability test was performed to select compounds 9 and 12, which had cytotoxicity of about 20% at a concentration of 40 μ M, and the experiment was conducted using these compounds.

Firstly, we tested whether the NHDC and derivatives inhibited the adipogenic differentiation. General markers used to identify adipogenic differentiation in hASCs

is the lipid accumulation which is measured by Oil Red O staining and the expression of PPAR- γ .³¹ We examined the expression of PPAR- γ , which plays an important role in adipogenic differentiation by regulating the expression of genes involved in adipocyte maturation.³² It has been reported that adipose-specific PPAR- γ knockout mice were fed a high-fat diet, but inhibited insulin resistance induced by high-fat diet and decreased body weight.³³ The increased amount of Oil red O staining and up-regulated expression of PPAR- γ observed in the differentiation group indicated the successful adipogenic differentiation of hASCs. In contrast, no specific adipogenic differentiation in control group had been observed from the Oil Red O staining and PPAR- γ expression data. Compound 9 and 12 treated groups showed reduced lipid accumulation and decreased expression of PPAR- γ at both the protein and transcription level (Fig. 5A to E).

SREBP-1, transcription factor that regulating fatty acid synthesis, had been used as a good indicator of lipogenic status of the cell. FAS which was one of the target enzyme of SREBP-1 condensed acetyl-CoA and malonyl-CoA to generate long fatty acids.³⁴ Because overexpressing SREBP-1 enhanced lipogenesis, up-regulated SREBP-1 level in Fig. 7A indicated the matured lipogenesis, which was correlated with differentiation markers such as Oil Red O staining and PPAR- γ expression. In other words, the expression of SREBP-1 implied lipogenesis in mature adipocytes. Thus, the result that decreases in expression of SREBP-1 in the compound 9, 12 treated group supported the inhibition ability of these compound on adipogenic differentiation.

Previous report showed that ROS mediated the adipogenic differentiation in 3T3-L1 cells. H_2O_2 , exogenous oxidative stress, induced adipogenic differentiation by transcriptional activation of CREB.³⁵ Based on the fact that adipogenic differentiation was caused by oxidative stress, we assumed that the higher intracellular ROS production could be observed in hASCs, when the cells were differentiated into adipocytes by a common adipogenic differentiation medium. As expected, flow cytometry result from differentiated hASC stained with DCFDA showed that the amount of ROS accumulated in cells increased as cells were differentiated into adipocytes. It can be concluded that the accumulation of intracellular ROS increases as adipogenic differentiation was proceeded in hASCs (Fig. 8). Because compounds 9 and 12 reduced the production of ROS and accumulation of lipid, these compounds appeared to inhibit the adipogenic differentiation by reducing ROS production.

Finally, Nrf2 known to the key transcriptional regulator of various antioxidant enzymes regulates the cellular ROS production.²³ We had already found that NHDC derivatives reduced intracellular ROS level in hASCs. The expression of Nrf2 was investigated in order to determine whether the amount of ROS production reduced by these compounds was mediated by the Nrf2 pathway. In accordance with previous data, compounds 9 and 12 showed up-regulation of Nrf2 in both the protein and transcriptional level, which resulted in the expression of the antioxidant enzymes such as HO-1 and NQO-1.

V. CONCLUSIONS

We demonstrated the NHDC derivatives inhibited adipogenic differentiation by regulation of ROS production through Nrf2 pathway. NHDC derivatives such as compounds 9 and 12 activated cytoprotective Nrf2 pathway. The activation of Nrf2 by these derivatives induced the expression of antioxidant enzymes including HO-1 and NQO-1, resulting in the reduction of ROS production during the adipogenic differentiation. Intraellular ROS production appeared to be key causal effector of adipogenic differentiation. Thus, NHDC derivatives, having strong effects on Nrf2 activation and ROS reduction in hASC, could be a potential therapeutic tool to overcome obesity. Especially, compound 9 seems to have stronger Nrf2 activation effect showing higher reduction of ROS production.

REFERENCES

1. Wang Y, Chen X, Song Y, Caballero B, Cheskin L. Association between obesity and kidney disease: a systematic review and meta-analysis. *Kidney international* 2008;73:19-33.
2. Bianchini F, Kaaks R, Vainio H. Overweight, obesity, and cancer risk. *The lancet oncology* 2002;3:565-74.
3. Janssen I. The public health burden of obesity in Canada. *Can J Diabetes* 2013;37:90-6.
4. Flegal KM, Carroll MD, Kit BK, Ogden CL. Prevalence of obesity and trends in the distribution of body mass index among US adults, 1999-2010. *Jama* 2012;307:491-7.
5. Shin H-Y, Kang H-T. Recent trends in the prevalence of underweight, overweight, and obesity in Korean adults: The Korean National Health and Nutrition Examination Survey from 1998 to 2014. *Journal of epidemiology* 2017;27:413-9.
6. Bondia-Pons I, Ryan L, Martinez JA. Oxidative stress and inflammation interactions in human obesity. *Journal of physiology and biochemistry* 2012;68:701-11.
7. Chamberlain G, Fox J, Ashton B, Middleton J. Concise review: mesenchymal stem cells: their phenotype, differentiation capacity, immunological features,

- and potential for homing. *Stem cells* 2007;25:2739-49.
8. Sawant A, Chanda D, Isayeva T, Tsuladze G, Garvey WT, Ponnazhagan S. Noggin is novel inducer of mesenchymal stem cell adipogenesis: implications for bone health and obesity. *J Biol Chem* 2012;287:12241-9.
 9. Sudo K, Kanno M, Miharada K, Ogawa S, Hiroyama T, Saijo K, et al. Mesenchymal progenitors able to differentiate into osteogenic, chondrogenic, and/or adipogenic cells in vitro are present in most primary fibroblast-like cell populations. *Stem Cells* 2007;25:1610-7.
 10. Janderova L, McNeil M, Murrell AN, Mynatt RL, Smith SR. Human mesenchymal stem cells as an in vitro model for human adipogenesis. *Obes Res* 2003;11:65-74.
 11. Nakamura T, Shiojima S, Hirai Y, Iwama T, Tsuruzoe N, Hirasawa A, et al. Temporal gene expression changes during adipogenesis in human mesenchymal stem cells. *Biochem Biophys Res Commun* 2003;303:306-12.
 12. Storz P. Forkhead homeobox type O transcription factors in the responses to oxidative stress. *Antioxid Redox Signal* 2011;14:593-605.
 13. Furukawa S, Fujita T, Shimabukuro M, Iwaki M, Yamada Y, Nakajima Y, et al. Increased oxidative stress in obesity and its impact on metabolic syndrome. *J Clin Invest* 2004;114:1752-61.
 14. Tormos KV, Anso E, Hamanaka RB, Eisenbart J, Joseph J, Kalyanaraman B,

- et al. Mitochondrial complex III ROS regulate adipocyte differentiation. *Cell Metab* 2011;14:537-44.
15. Owusu-Ansah E, Banerjee U. Reactive oxygen species prime *Drosophila* haematopoietic progenitors for differentiation. *Nature* 2009;461:537-41.
 16. Horton JD, Goldstein JL, Brown MS. SREBPs: activators of the complete program of cholesterol and fatty acid synthesis in the liver. *The Journal of clinical investigation* 2002;109:1125-31.
 17. Platt ID, El-Sohemy A. Regulation of osteoblast and adipocyte differentiation from human mesenchymal stem cells by conjugated linoleic acid. *J Nutr Biochem* 2009;20:956-64.
 18. Yu WH, Li FG, Chen XY, Li JT, Wu YH, Huang LH, et al. PPARgamma suppression inhibits adipogenesis but does not promote osteogenesis of human mesenchymal stem cells. *Int J Biochem Cell Biol* 2012;44:377-84.
 19. Nguyen T, Nioi P, Pickett CB. The Nrf2-antioxidant response element signaling pathway and its activation by oxidative stress. *J Biol Chem* 2009;284:13291-5.
 20. Saw CL-L, Wu Q, Kong A-N. Anti-cancer and potential chemopreventive actions of ginseng by activating Nrf2 (NFE2L2) anti-oxidative stress/anti-inflammatory pathways. *Chinese Medicine* 2010;5:37.
 21. He X, Ma Q. NRF2 cysteine residues are critical for oxidant/electrophile-

- sensing, Kelch-like ECH-associated protein-1-dependent ubiquitination-proteasomal degradation, and transcription activation. *Mol Pharmacol* 2009;76:1265-78.
22. Li W, Thakor N, Xu EY, Huang Y, Chen C, Yu R, et al. An internal ribosomal entry site mediates redox-sensitive translation of Nrf2. *Nucleic Acids Res* 2010;38:778-88.
23. Lee JH, Khor TO, Shu L, Su ZY, Fuentes F, Kong AN. Dietary phytochemicals and cancer prevention: Nrf2 signaling, epigenetics, and cell death mechanisms in blocking cancer initiation and progression. *Pharmacol Ther* 2013;137:153-71.
24. Benavente-Garcia O, Castillo J. Update on uses and properties of citrus flavonoids: new findings in anticancer, cardiovascular, and anti-inflammatory activity. *J Agric Food Chem* 2008;56:6185-205.
25. Choi JM, Yoon BS, Lee SK, Hwang JK, Ryang R. Antioxidant properties of neohesperidin dihydrochalcone: inhibition of hypochlorous acid-induced DNA strand breakage, protein degradation, and cell death. *Biol Pharm Bull* 2007;30:324-30.
26. Lo Furno D, Graziano ACE, Avola R, Giuffrida R, Perciavalle V, Bonina F, et al. A Citrus bergamia Extract Decreases Adipogenesis and Increases Lipolysis by Modulating PPAR Levels in Mesenchymal Stem Cells from Human

- Adipose Tissue. *PPAR Research* 2016;2016:9.
27. Hofbauer KG, Nicholson JR, Boss O. The obesity epidemic: current and future pharmacological treatments. *Annu Rev Pharmacol Toxicol* 2007;47:565-92.
 28. Shin S, Wakabayashi N, Misra V, Biswal S, Lee GH, Agoston ES, et al. NRF2 modulates aryl hydrocarbon receptor signaling: influence on adipogenesis. *Mol Cell Biol* 2007;27:7188-97.
 29. Xu J, Kulkarni SR, Donepudi AC, More VR, Slitt AL. Enhanced Nrf2 activity worsens insulin resistance, impairs lipid accumulation in adipose tissue, and increases hepatic steatosis in leptin-deficient mice. *Diabetes* 2012;61:3208-18.
 30. Zhang D-y, Pan Y, Zhang C, Yan B-x, Yu S-s, Wu D-l, et al. Wnt/ β -catenin signaling induces the aging of mesenchymal stem cells through promoting the ROS production. *Molecular and Cellular Biochemistry* 2013;374:13-20.
 31. Dionisi M, Alexander S, Bennett A. Oleamide activates peroxisome proliferator-activated receptor gamma (PPAR) in vitro; 2012.
 32. Farmer SR. Regulation of PPARgamma activity during adipogenesis. *Int J Obes (Lond)* 2005;29 Suppl 1:S13-6.
 33. Jones JR, Barrick C, Kim KA, Lindner J, Blondeau B, Fujimoto Y, et al. Deletion of PPARgamma in adipose tissues of mice protects against high fat diet-induced obesity and insulin resistance. *Proc Natl Acad Sci U S A*

- 2005;102:6207-12.
34. Horton JD, Shah NA, Warrington JA, Anderson NN, Park SW, Brown MS, et al. Combined analysis of oligonucleotide microarray data from transgenic and knockout mice identifies direct SREBP target genes. *Proc Natl Acad Sci U S A* 2003;100:12027-32.
 35. Kanda Y, Hinata T, Kang SW, Watanabe Y. Reactive oxygen species mediate adipocyte differentiation in mesenchymal stem cells. *Life Sci* 2011;89:250-8.

ABSTRACT(IN KOREAN)

네오헤스페리딘 다이하이드로찰콘과 그 유도체의 Nrf2 경로를 통한
인간 지방유래 줄기세포의 지방 분화 억제효과

<지도교수 인요한>

연세대학교 대학원 의학과

강희택

배경: 비만은 전세계적으로 유행하는 질병이다. 비만의 병태생리는 복잡하지만 열량섭취 증가와 신체활동 감소가 주된 원인이지만 산화스트레스와 염증반응도 주요한 원인으로 알려져 있다. 특히 활성산소는 지방세포 분화에 관여하는 주요 원인이다. 네오헤스페리딘은 강력한 항산화물질 중 하나로 라디칼을 제거하고 항염증작용을 갖는다. 그러나 네오헤스페리딘 다이하이드로찰콘 (Neohesperidine dihydrochalcone, NHDC)과 그 유도체가 지방세포 분화와 비만 발생에 어떠한 영향을 미치는지는 알려지지 않았다.

목적: 본 연구는 NHDC와 그 유도체가 지방유래 줄기세포의 지방세포 분화 과정에 억제 효과를 갖는지 알아보기 위해 진행되었다.

방법: 지방유래 줄기세포는 성장인자와 L-글루타민이 보충된 배지에서 배양되었다. 배양액은 매 3일마다 바뀌었으며, 4-7세대의 조기 세포 패시지(passage)가 사용되었다. 지방유래 줄기세포에 대한 NHDC와 유도체의 세포독성을 측정하였다. 지방유래 줄기세포는 증식배지와 분화배지에서 NHDC와 유도체의 투여 후 각각 배양되었다. 대조군은 NHDC와 유도체를 모두 투여하지 않고 증식배지에서 배양, 분화군은 NHDC와 유도체를 모두 투여하지 않고 증식배지와 분화배지에서 배양,

실험군은 NHDC 또는 유도체 중 하나를 투여한 후 증식배지와 분화배지에서 배양하였다. 세포 내 지방축적은 Oil Red O 염색을 이용해 측정했다. 지방분화 표지자의 발현정도는 RT-PCR과 Western blot을 이용하여 측정하였다.

결과: NHDC와 유도체 9번, 12번을 처리한 집단에서 분화군보다 지방축적이 적게 관찰되었다. PPAR- γ 발현도 유도체 9번, 12번을 처리한 집단에서 분화군보다 각각 46.7%와 70%씩 감소하였다. FAS 발현도 유도체 9번, 12번을 처리한 집단에서 51.6%와 38.5%씩 감소하였다. 또한 유도체 9번, 12번 처리하였을 때 SREBP-1의 발현도 65.7% 및 60%씩 감소하였다. NHDC와 유도체 12번을 처리한 집단에서 활성산소 발생이 분화군보다 감소하지 않았지만, 유도체 9번을 처리한 집단에서 활성산소의 감소가 크게 나타났다. Nrf2 발현이 NHDC 및 유도체 9번을 처리한 집단에서 통계적으로 의미있게 변화하지 않았지만, 유도체 12번을 처리한 집단에서는 Nrf2 발현량이 크게 증가했다. 또한 Nrf2의 항산화작용의 하위단계에서 발현되는 HO-1 및 NQO-1의 상대적 발현량도 NHDC와 유도체 9번 및 12번에서 증가되었다.

결론: NHDC 유도체는 Nrf2 경로를 활성화시켜 활성산소 발생을 억제시키고 지방유래 줄기세포의 지방세포 분화를 억제한다. 특히 유도체 9번은 Nrf2 경로를 더욱 강하게 활성화시켜 활성산소의 생성 감소를 유도한다.

핵심되는 말: 네오헤스페리딘; 지방분화; 줄기세포; 활성산소; Nrf2